

GAS TURBINE DESIGN AND MATCHING RESEARCH OF WASTE HEAT RECOVERY SYSTEM FOR MARINE DIESEL ENGINE

Jiewei Peng, Zijian Zhang, Zhichao Gu, Peijun Qin

*Shanghai Marine Diesel Engine Research Institute
Shanghai, China
pengjiewei_yi@163.com*

** Jiewei Peng*

ABSTRACT

With the emphasis on energy and environmental protection, energy-conservation and emission-reduction become vital issues for industrial development. Moreover, with the development of legislation on marine environment, the marine diesel engine has become focusing on energy saving and emission reduction for ships. For low-speed diesel engines under high load, waste heat from exhaust gas can be recovered by the compact and efficient gas turbine.

In this paper, the matching design research between low speed diesel engine and gas turbine is carried out. To balance efficiency and compactness, the impeller was adjusted and generated by ANSYS BLADEGEN, based on 1D thermodynamic design. And the 1D calculation is similar to the CFX simulation result: the total-static efficiency is 73.8% compare to 76.7%.

Moreover, the flow separation was happened at the impeller suction side and created vortex due to the high incidence angle. The off-design operating point simulation of the turbine shows though the pressure ratio increase will cause the efficiency decline a little, the total shaft power rises.

In sum, this paper worked out a power turbine suitable for a low-speed diesel engine according to the turbine character matching design and simulation, which provides foundation to the construction of a steady operation waste heat recovery system for marine diesel engine.

1. INTRODUCTION

With the rising of fuel price and the increasing voice of global energy saving and emission reduction, a more efficient and convenient energy recycling method is deadly in needed. According to the statistics, about 50% of the heat generated by marine diesel engine was exhausted in the form of waste gas, therefore, effective recovery and utilization of exhaust heat from marine diesel engine is significant for improving the efficiency of heat utilization and reducing the environmental pollution caused by exhaust emissions.

At present, the major wasted heat recovery technologies are mainly as followed: turbocharging, turbo compound generator (also called turbocompounding), Brayton cycle, Rankine engine cycle and thermoelectric generators (Zhao et al., 2014; Edwards et al., 2010; Shu et al., 2013; Rahbar et al., 2015; Kim et al., 2019; Teo et al., 2019; Yang et al., 2019). Among them, the turbocompounding technology convert the waste energy into electric or mechanical energy by gas turbine. Aghaali and Angstrom (2015) compared different recovery technologies and concluded turbocompounding can not only decrease

brake specific fuel consumption (BSFC), but also simplify the structure so as to reduce the volume. Based on the expansion ratio of power turbine, that paper divided the turbocompounding into low-pressure turbocompounding (LP) and high-pressure turbocompounding (HP). In addition, different kinds of integration and structure of turbocompoundings have been analyzed, proving that the turbocompounding configuration affect both the performance of the power turbine and the operating characteristics of the diesel engine (Wei et al, 2010; Hopmann and Algrain, 2003).

Apart from the configuration of turbocompounding system, the design of power turbine is the core aspect of waste heat recovery. Mamat et al. (2011) designed a turbine with a low expansion ratio (1.1), whose exit-to-inlet area ratio is much smaller than the empirical value. In order to improve the turbine efficiency, Alshammari et al. (2017) adopted a non-zero blade angle.

In this paper, a low-speed diesel engine is taken as the research object, and the matching design of power turbine is carried out. In order to improve the compactness of the 100 kW class power turbine designed by this paper, the structure design and optimization of the turbine were carried out, and the multi-condition aerodynamic simulation analysis was carried out by CFX.

2. 1D THERMODYNAMIC DESIGN

2.1 Turbine matching

The power turbine in this thesis is designed according to a low speed diesel engine. This type of diesel engine parameters at 100% load are as follows: exhaust flow rate is 8.79 kg/s, exhaust temperature is 392 °C, exhaust pressure is 382 kPa. In order to recover the heat without impacting the diesel engine, turbocompounding is parallel connection with the turbocharger. The matching data between diesel engine and power turbine is obtained by calculation, as shown in Table 1.

It shows that under 100% loading, the power turbine can recover 145.9 kW electric energy when bypassing 0.76 kg/s exhaust gas, while the system energy recycling rate is about 1.32%. Therefore the input parameter of the power turbine could be set as shown in Table 2.

Table 1: Load characteristics of power turbine waste heat recovery system

(Parameter definitions: Turbine energy recovery rate = Turbine power / Diesel power; System energy recovery rate = (Turbine power + Diesel power – Original diesel power) / Low calorific value)

| Load | 50% | 75% | 85% | 100% |
|---------------------------------|--------|--------|--------|--------|
| Diesel Power/kW | 2170.6 | 3138.4 | 3626.6 | 4235.5 |
| Turbine Power /kW | 35.3 | 90.7 | 108.1 | 145.9 |
| Turbine energy recovery rate /% | 1.63 | 2.89 | 2.98 | 3.44 |
| System energy recovery rate /% | -2.33 | 0.54 | 0.78 | 1.32 |
| Bypass flow /kg·s ⁻¹ | 0.41 | 0.62 | 0.68 | 0.80 |

Table 2: Power turbine design parameters

| | |
|--------------------------------------|-------|
| Inlet pressure /kPa | 380 |
| Inlet temperature /°C | 480 |
| Exit pressure /kPa | 101.3 |
| Exhaust gas flow /kg·s ⁻¹ | 0.8 |

2.2 1D calculation

The expansion ratio of the power turbine is about 3.75, which is low to a radial turbine. Thus, the subsonic guide vane was utilized to improve aerodynamic performance of the stator and the adaptability of the turbine at various operating point. The Mach number M_3 at the exit of stator is less than 0.95. According to the research findings made by Institute of Mechanics, CAS (shown in Figure 1), lower Mach number may cause a higher energy loss, which would worsen the stator performance. Thus, the M_3 above 0.7 is adopted in this paper.

According to the reference (Li and Lu, 1987), the energy losses are mainly as follows in the Table 3.

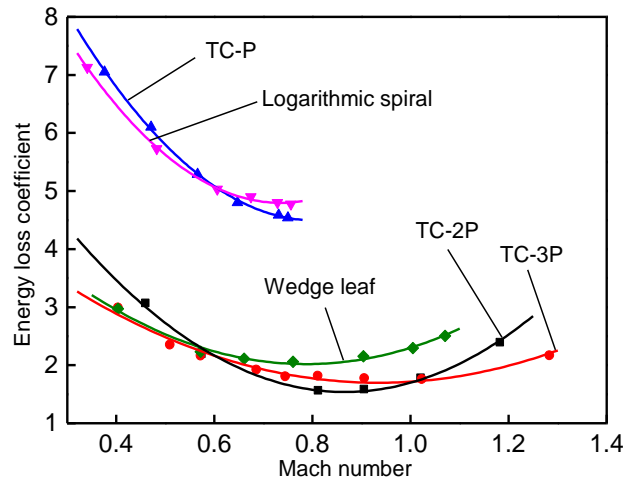


Figure 1: Comparison of aerodynamic performance of several guide vanes

Table 3: Mainly energy loss coefficients for power turbine

| | | | |
|--------------------------------------|--|--|---|
| Wheel friction loss power | $N_f = f \rho_4 D_4^2 \left(\frac{u_4}{100}\right)^3 \frac{1}{1.36}$ | Impeller inlet blocking factor | $\tau_4 = 1 - \frac{Z_r \Delta_4}{\pi D_4 \sin \beta_{4b}}$ |
| Impeller exit blocking factor | $\tau_5 = 1 - \frac{\Delta_5 Z_r}{\pi D_5 \sin \beta_{5b}}$ | Relative residual loss | $\zeta_{c5} = \left(\frac{c_5}{c_a}\right)^2$ |
| Leakage loss coefficient | $\eta_\Delta = 1 - 1.3 \cdot \frac{\Delta_r}{l_m}$ | Partial Intake Loss Coefficient | $\eta_e = 1 - \left(\frac{0.27}{\sqrt{e}} - 0.27\right)$ |

In Table 3:

f : friction loss coefficient

D_4 : impeller inlet diameter, m

Z_r : number of rotor blade

D_5 : impeller exit diameter, m

c_5 : absolute exit velocity, m/s

Δ_r : impeller tip radial clearance, m

e : partial intake coefficient

ρ_4 : exhaust density at impeller inlet, kg/m³

u_4 : rotor blade speed at the inlet, m/s

Δ_4 : mean blade thickness at impeller inlet, m

β_{5b} : impeller exit blade angle, °

c_a : ideal expansion velocity, m/s

l_m : mean impeller blade height, m

2.3 Optimization of 1D calculation results

The paper has designed three turbine cases as shown in Table 4. The case 1 provide a turbine with 30000rpm and impeller diameter 266.6mm, which offer a total-static efficiency of 79.7% and a shaft power of 142.3 kW. However, case 1 results in an excessively large impeller diameter, thus the case 2

was worked out to improve it.

In case 2 the impeller diameter is reduced to 149.3 mm by raising the rotating speed and optimizing some structure. Comparing case 1 and case 2, although the total-static efficiency in case 2 is lower, the wheel friction loss is not higher (17.6 kW in case 1 and 4.7 kW in case 2). Due to its lower velocity ratio and impeller diameter, the shaft power in case 2 is similar to case 1.

Nonetheless, the raising of the rotating speed in case 2 causes a series of other design difficulties as: shaft design, seal design, bearing and generator selection. With the aim of limiting the rotating speed under 30000 rpm, the case 3 was worked out by decreasing the velocity ratio to 0.46, which shorten the impeller diameter to 76.7% compare to the case 1. Though the total-static efficiency was lowered, the shaft power is still acceptable as 128.7 kW.

Therefore, regard the rotational speed, size and efficiency, the paper take case 3 as the most balancing design, whose data based on the 3D flow channel design of the turbine.

Table 4: Comparison of 1D design case of power turbine

| Parameters | Case 1 | Case 2 | Case 3 |
|-------------------------|--------|--------|--------|
| Rotational speed /rpm | 30000 | 50000 | 30000 |
| Velocity ratio | 0.60 | 0.56 | 0.46 |
| Impeller diameter /mm | 266.6 | 149.3 | 204.4 |
| Reaction | 0.55 | 0.60 | 0.60 |
| Inlet absolute angle /° | 18.11 | 20 | 18.11 |
| Incidence angle /° | -3.04 | -2.94 | 10.84 |
| Wheel diameter ratio | 0.4 | 0.5 | 0.4 |
| Exit blade angle /° | 30 | 35 | 30 |
| Total-static efficiency | 0.797 | 0.692 | 0.738 |
| Shaft power /kW | 142.3 | 141.5 | 128.7 |

3. DETAILED DESIGN OF TURBINE

The stator blade exit Mach number is about 0.866 calculated by 1D model. As shown in Figure 1, TC-2P blade shape is the most suitable as its energy loss efficiency is the least under such circumstance. The stator's 3D model is shown in Figure 3.

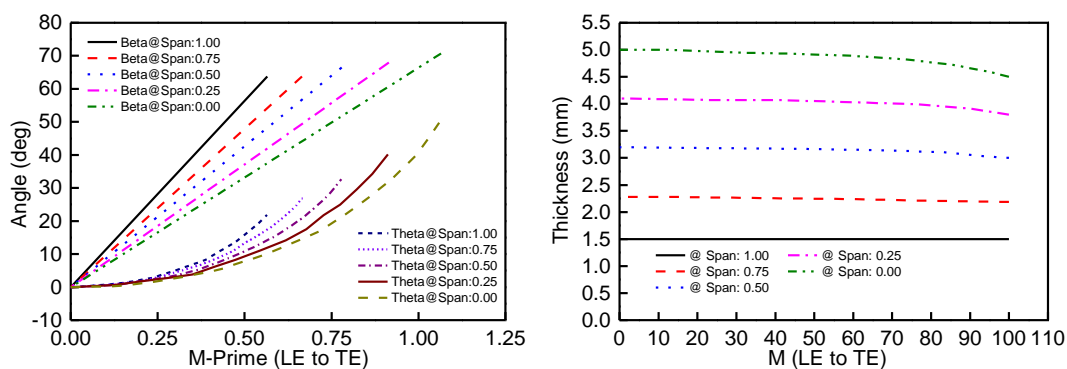


Figure 2: Layered distribution of rotor blade angle and thickness

The rotor designed by controlling mean camber line and blade thickness, the mean camber line is defined mainly by blade angle and enveloping angle, the blade surface is defined mainly by mean camber line and blade thickness. Figure 2 shows a plot of blade angle or thickness versus normalized meridional coordinate from leading edge to trailing edge.

Furthermore, the impeller tip clearance should be considered as well, because it dramatically influence the turbine efficiency and furthermore, the safety. Regard the impeller would expand under high temperature, the radial and axial clearance are both set to 0.5mm.

From what has been discussed above, the turbine detailing design data are shown in Table 5.

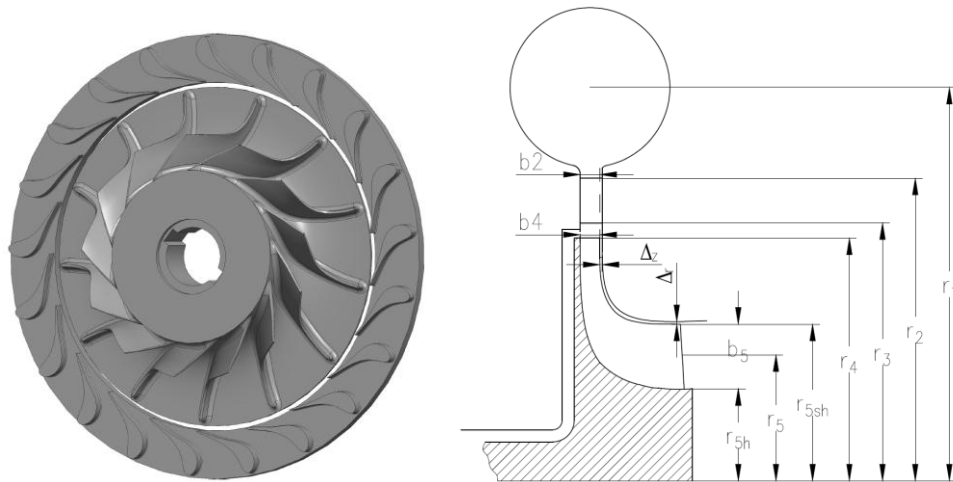


Figure 3: Geometries of the stator and rotor and the turbine parameters

Table 5: Turbine geometric parameters

| Input conditions | | Volute | | Stator | | Rotor | |
|------------------|-----------|--------|--------|--------------|----------|--------------|-----------|
| T_1 | 753.15 K | r_1 | 180 mm | vane | TC-2P | r_4 | 102.75 mm |
| p_1 | 380 kPa | M_v | 0.068 | r_2 | 138.5 mm | b_4 | 6.8 mm |
| G | 0.8 kg/s | | | b_2 | 6.8 mm | β_{4b} | 90° |
| p_5 | 101.3 kPa | | | r_3 | 108.5 mm | r_{5sh} | 75.95 mm |
| | | | | b_3 | 6.8 mm | r_{5h} | 53.7 mm |
| | | | | Z_s | 21 | b_5 | 22.25 |
| | | | | α_3 | 18.11 | β_{5b} | 30 |
| | | | | M_3 | 0.866 | Z_r | 13 |
| | | | | O_{throat} | 9.7 mm | Δ_r | 0.5 mm |
| | | | | | | Δ_z | 0.5 mm |

4 AERODYNAMIC SIMULATION

4.1 3D flow field analysis

After detailing design as above, the 3D model of the turbine was constructed by ANSYS Bladegen. Through the grid-independent verification, the meshed results are shown in Figure 4.

The simulation results under design point is simulated by CFX and shown in Figure 5 and Figure 6, which give the temperature, pressure, velocity at 50% spanwise. The contours and pressure distribution curves show that the flow accelerate gently at forehead while fiercely at the throat, and deflects under

the guidance of the vane. Correspondingly, the temperature and pressure changed gently at the beginning and then lowered dramatically.

Meanwhile the velocity decreases slightly at the gap between stator and rotor, showing the flow mixed in the gap. Such mixture makes the gas tend to be even at the inlet of rotor and contributes to the noise reduction and erosion prevention.

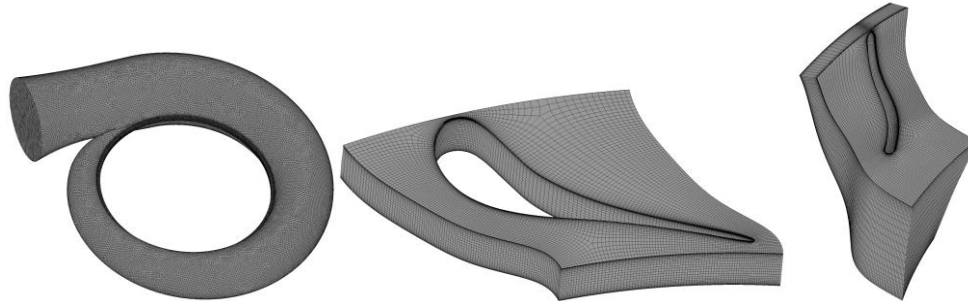
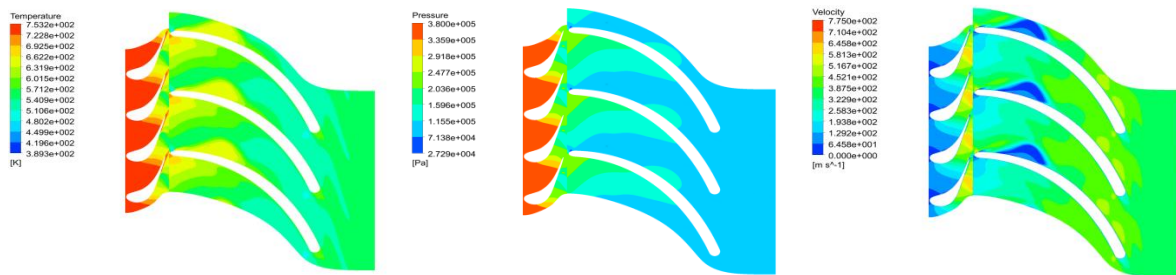


Figure 4: Meshed volute, stator and rotor

Moreover, the flow separation was happened at the impeller suction side, and thus created vortex. This is mainly due to the reduction of impeller diameter according to the case 3 in Table 4. The positive incidence angle at 10.84° , which directly causing the flow separation on the impeller blade suction side. As a result, the turbine efficiency is declined by additional energy losses.



(a) Temperature (b) Pressure (c) Velocity

Figure 5: The contours of temperature, pressure and velocity at 50% spanwise

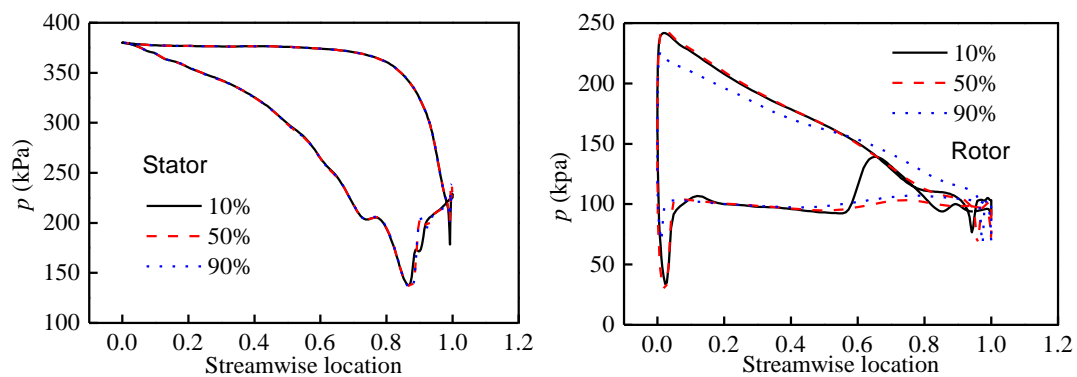


Figure 6: Stator and rotor blade pressure distribution at 10%, 50% and 90% streamwise

As shown in Figure 6, the pressure at the rotor blade pressure side change smoothly and gently, proving the steady and continuous work on the impeller. On the other side, due to the flow separation, the suction side exists a 28 kPa low pressure area, nevertheless, the pressure recovered rapidly and keep stable. Moreover, under the forces driven by hub and rotor blades, the gas was deflected causing pressure

increased to 139 kPa at 10% spanwise.

4.2 Off-design operating point simulation

In order to analyze the turbine working character under off-design operating point, the paper simulate different gas flow and rotational speed under turbine inlet temperature 480 °C and exit pressure 103.4 kPa. The rotational speed ranges from 26000 to 32000 rpm, and the mass flow ranges from 0.5 to 0.85 kg/s.

As shown in Figure 7(a), it's easy to conclude that the specific flow rate G_s increases as pressure ratio p_s raises, while the specific speed n_s increase as p_s decrease.

In addition, as can be seen from Figure 7(b), the turbine efficiency curves at each n_s are approximately parallel to each other. The decreasing of p_s or increasing of n_s , causes a lower incidence angle, which reduce the energy loss due to the flow separation, thus helps to improve turbine efficiency. Therefore, in the process of working with diesel engine, turbine's output power could be increased effectively when the exhaust pressure increases, but the power turbine efficiency would decreases slightly (p_s increases by 0.1 as η_{ts} decreases by about 0.2%).

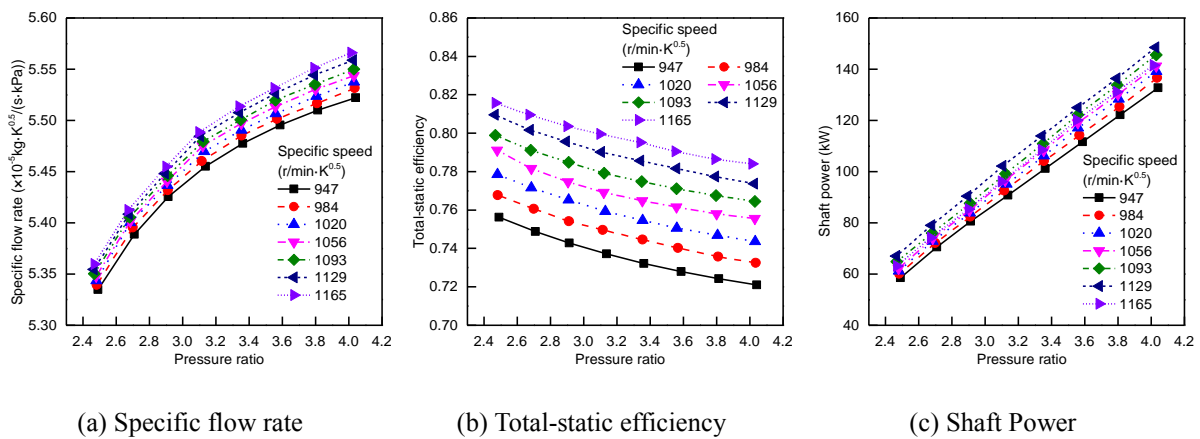


Figure 7: Characteristic curves of power turbine for off-design operating point

According to the power characteristic curves as shown in Figure 7(c), the turbine shaft power increase with the specific speed as the rotational speed varies from 947~1129, however, the power drops significantly while the specific speed continues to increase to 1165. This means that to ensure maximum turbine power, there is an optimum value for specific speed, about 1129. The optimum specific speed corresponds to 30000 rpm at 480 °C.

5. CONCLUSIONS

In order to recover the exhaust gas and improve the heat utilizing efficiency, this paper analyzed the matching character between one type of low-speed diesel engine and the power turbine by one dimension calculation. By comparing three design cases and balancing the efficiency and compactness, part of efficiency was sacrificed so as to reduce the speed ratio to 0.46 and impeller diameter reduce 23.3% (compare to the original case1).

Furthermore, this paper made detailing structure designed aided by ANSYS based on the one dimension design. The 3D aerodynamic simulation is analyzed by CFX. The simulation shows that in the stator gas flow accelerate gently at forepart while fiercely during the throat and deflected under guidance of vanes, meanwhile the flow separation was happened at the impeller suction side and created

vortex which is mainly due to the high incidence angle.

Totally the inside flow field of the turbine is smoothly and averagely, which meets the requirement. The off-design operating point simulation of the turbine shows though the pressure ratio increase will cause the efficiency decline a little, the total shaft power rises. On the other side when the turbine work on 30000 rpm, it possesses the optimum shaft power and efficiency.

REFERENCES

- Aghaali H., Angstrom H., 2015. A Review of Turbocompounding as a Waste Heat Recovery System for Internal Combustion Engines. *Renewable and Sustainable Energy Reviews*, vol. 49: p.813-824.
- Alshammari F., Karvountzis-Kontakiotis A., Pesiridis A., 2017. Radial Expander Design for an Engine Organic Rankine Cycle Waste Heat Recovery System. *Energy Procedia*, vol. 129: p. 285-292.
- Edwards K. D., Wagner R. M., Briggs T., 2010. Investigating Potential Light-duty Efficiency Improvements through Simulation of Turbo-compounding and Waste-heat Recovery Systems. *SAE Technical Papers*, 2019-01-2209.
- Hopmann U., Algrain M. C., 2003. Diesel Engine Electric Turbo Compound Technology. *SAE Int.*, 2003-01-2294.
- Hountalas D. T., Katsanos C. O., Lamaris V. T., 2007. Recovering Energy from the Diesel Engine Exhaust Using Mechanical and Electrical Turbocompounding. *SAE Int.*, 2007-01-1563.
- Hudong Shipbuilding Manufacturing Technology Group, 1978. Compressor Modeling Test of GZ750 Turbocharging. Institute of Mechanics, Chinese Academy of Sciences.
- Kim J., Kim D., Kim Y., 2019. Experiment on Radial Inflow Turbines and Performance Prediction Using Deep Neural Network for the Organic Rankine Cycle. *Applied Thermal Engineering*, vol. 149: p. 633-643.
- Li Y., Lu G., 1987. Centripetal Turbine and Centrifugal Compressor. China Machine Press, Beijing, China.
- Lu G., 1984. Determination of Airflow Parameters in Radial Leafless Space. *Shanghai Jiaotong University Technology*, no. 4.
- Mamat A. M. I., Padzillah M. H., Romagnoli A., et al, 2011. A High Performance Low Pressure Ratio Turbine for Engine Electric Turbocompounding. *ASME paper*, GT2011-45541.
- Rahbar K., Mahmoud S., Al-dadah R., et al, 2015. Preliminary Mean-line Design and Optimization of a Radial Turbo-Expander for Waste Heat Recovery Using Organic Rankine Cycle. *Energy Procedia*, vol. 75: p. 860-866.
- Shu G., Liang Y., Wei H., et al, 2013. A Review of Waste Heat Recovery on Two-Stroke IC Engine Aboard Ships. *Renewable and Sustainable Energy Reviews*, vol. 19: p. 385-401.
- Teo A., Chiong M., Yang M., et al, 2019. Performance Evaluation of Low-Pressure Turbine, Turbo-Compounding and Air-Brayton Cycle as Engine Waste Heat Recovery Method. *Energy*, vol. 166, no. 1: p. 895-907.
- Wei W., Zhuge W., Zhang Y., et al, 2010. Comparative Study on Electric Turbo-Compounding Systems for Gasoline Engine Exhaust Energy Recovery. *ASME paper*, GT2010-23204.
- Yang Y., Wang S., He W., 2019. Simulation Study on Regenerative Thermoelectric Generators for Dynamic Waste Heat Recovery. *Energy Procedia*, vol. 158, p. 571-576.
- Zhao R., Zhuge W., Zhang Y., et al, 2014. Parametric Study of Power Turbine for Diesel Engine Waste Heat Recovery. *Applied Thermal Engineering*, vol. 64: p. 308-319.